PERGAMON

International Journal of Heat and Mass Transfer 42 (1999) 2111–2117

International Journal of HEAT and MASS TRANSFER

Technical Note

Buoyant convection in a non-rectangular cavity with non-vertical insulating sidewalls

G.B. Kim, J.M. Hyun*

Department of Mechanical Engineering, Korea Advanced Institute of Science and Technology, Taejon 305-701, South Korea

Received 6 February 1998; in final form 28 July 1998

1. Introduction

Consider a vertically-mounted rectangular enclosure (width L and height H), filled with a viscous, Boussinesq fluid. The top and bottom horizontal walls are thermal conductors, maintained at temperatures T_H and T_C, with $\Delta T \equiv (T_H - T_C)/2 > 0$, respectively. If the vertical sidewalls are thermally insulated, there are no fluid motions, and heat transfer is strictly conductive. Consequently, the appropriately-defined average conventional Nusselt number $\overline{Nu}$ at the horizontal wall is unity. The present setup is top-heated, and it should be distinguished from the bottom-heated Benard-type configuration with $\Delta T < 0$. One key ingredient in the present arrangement is the fact that the insulating sidewalls are straight and vertical everywhere. The insulating condition calls for the vanishing of local temperature gradient in the normal direction of the boundary wall. In this case, the conduction-controlled isotherms (hence, iso-density lines) are horizontal and equi-spaced everywhere, and the fluid in the entire cavity is stably stratified with a linear density profile in the vertical direction. This implies that, at the vertical sidewalls, the condition that the isotherms are locally perpendicular to the wall is trivially satisfied. Furthermore, the pressure distribution is determined by hydrostatic relation, and the resulting isobars and iso-density lines are parallel. In this connection, the so-called baroclinic term in the vorticity equation, i.e., $(\nabla p \times \nabla \rho)/\rho^2$, is identically zero, and the whole cavity is vorticity-free.

If portions of the sidewalls are warped and/or non-vertical, the static equilibrium of the previous case will have to be modified fundamentally. Since the sidewalls are thermally insulated, i.e., $\partial T/\partial n = 0$ at the wall where n denotes the normal direction, the isotherms (hence, iso-density lines) near the non-vertical wall sections should meet the wall locally perpendicularly. If the pressure distributions are still largely hydrostatic, the iso-density lines and isobars are not exactly parallel in these regions, which leads to a non-vanishing baroclinic term, i.e., $(\nabla p \times \nabla \rho)/\rho^2 \neq 0$. The consequence is that vorticity is generated in these localized regions, which points to the initiation of fluid motions. As can be easily understood, even if the sidewalls are insulated, the existence of non-vertical portions of the sidewall gives rise to convective activities. It follows that, because of convective fluid flows, the overall heat transfer from the top to bottom horizontal walls of this case will be augmented compared to the purely conductive case. This simplistic idea can be exploited as a possible device to add an element of baroclinically-induced natural convective heat transfer in an otherwise conduction-dominated fluid in an enclosure.

There exists a vast collection of technical literature on confined natural convection [1–2] and studies on various cases involving a non-rectangular enclosure are numerous for a trapezoidal enclosure [3–7], and for a parallelogram-shaped cavity [8–10]. In the flow configuration of these preceding studies, the horizontal walls are insulators and the sidewalls are thermal conductors on which constant temperatures are imposed. As remarked earlier, the impetus of the present configuration lies in the presence of non-vertical segments of thermally-insulating sidewalls. The focus is on the explicit role of local baroclinicity induced in the close neighborhood of non-vertical portions of the sidewalls.

2. Problem formulation

Flow is governed by the Navier-Stokes equations with the Boussinesq fluid approximation, which, after non-dimensionalization, reads:

* Corresponding author

0017–9310/99/$ - see front matter
PII: S0017–9310(98)00312–3

$$\frac{\partial U}{\partial X}+\frac{\partial V}{\partial Y}=0 \tag{1}$$

$$U\frac{\partial U}{\partial X}+V\frac{\partial U}{\partial Y}=-\frac{\partial P}{\partial X}+\frac{\partial}{\partial X}\left(Pr\frac{\partial U}{\partial X}\right)+\frac{\partial}{\partial Y}\left(Pr\frac{\partial U}{\partial Y}\right) \tag{2}$$

$$U\frac{\partial V}{\partial X}+V\frac{\partial V}{\partial Y}=-\frac{\partial P}{\partial Y}+\frac{\partial}{\partial X}\left(Pr\frac{\partial V}{\partial X}\right)+\frac{\partial}{\partial Y}\left(Pr\frac{\partial V}{\partial Y}\right)+Ra\cdot Pr\cdot\theta \tag{3}$$

$$U\frac{\partial \theta}{\partial X}+V\frac{\partial \theta}{\partial Y}=\frac{\partial^2\theta}{\partial X^2}+\frac{\partial^2\theta}{\partial Y^2} \tag{4}$$

In the preceding equations, dimensionless quantities are defined as

$$(X, Y)=(x, y)/H;\quad (U, V)=(u, v)/(\kappa/H); P=pH^2/\rho_0\kappa^2;$$

$$\theta=(T-T_0)/\Delta T;\quad Pr=\nu/\kappa;\quad Ra=g\beta\Delta TH^3/\nu\kappa,$$

in which, (u, v) denote velocity components in the horizontal (x) and vertical (y) directions, ρ_0 and T_0 refer respectively to the center-point reference density and temperature in the Boussinesq fluid relation $\rho=\rho_0[1-\beta(T-T_0)]$, ν and κ the kinetic viscosity and thermal diffusivity, and β the coefficient of thermometric expansion of the fluid. The fluid properties are taken to be constant.

The associated boundary conditions are expressed as

$U=V=0$ at all solid walls;

$\theta=\pm 1.0$ at the top and bottom horizontal endwalls, respectively;

$\dfrac{\partial\theta}{\partial n}=0$ at the sidewalls.

Obviously, the governing equations and boundary conditions are standard and highly regularized. The numerical solution procedure for this type of problem is well established, and the widely-utilized SIMPLE algorithm [11] was adopted. A body-fitted coordinate transform was implemented. For most calculations, an (80×80) staggered and stretched grid was deployed to cluster mesh points near the walls. A series of computations were repeated for benchmark problems to verify the reliability and resolution of the code. Grid-convergence tests were performed for a variety of cavity shape and flow conditions, and the outcome proved that the numerical methodologies used were robust and accurate.

3. Results and discussion

All the computations were conducted for $Pr=7.0$ to simulate water.

First, the results pertinent to the parallelogram-shape are shown in Fig. 1. The nominal aspect ratio $Ar\,[=H/L]$ is fixed at 1.0, and the specific geometry is determined by the incline angle ϕ of the insulated sidewall.

Figure 1 exhibits exemplary plots of stream function ψ and temperature θ. Here ψ is defined such that

$$u=\frac{\partial\psi}{\partial y},\quad v=-\frac{\partial\psi}{\partial x}.$$

For high Ra, the main flow is characterized by a counterclockwise circulation cell. It is conspicuous that, as Ra increases, the fluid motion is concentrated in thin boundary layers, and in the interior core, the fluid is largely stagnant and is almost linearly stratified in the vertical direction. Notice that the boundary layer on the sidewall drives the motion, and the boundary layer on the horizontal wall is passive, in that it provides a passageway for the flow. In much of the interior, isotherms are horizontal; only in narrow regions in the immediate vicinity of the slanted sidewall, isotherms deviate from the horizontal direction. As emphasized previously, these locally non-horizontal isotherms generate flow.

The above general trends are more pronounced as the incline angle ϕ or Ra increases.

The enhancement of heat transfer is discernible in the plot of local Nusselt number Nu

$$\left[\equiv\frac{1}{2}\frac{\partial\theta}{\partial Y}\bigg|_{Y=0}\right]$$

at the bottom horizontal endwall, as exhibited in Fig. 2(a). In comparison to the case of a rectangular cavity ($\phi=0^\circ$) for which Nu is uniformly 1.0, augmentation of Nu is evident as ϕ increases. As illuminated in the flow pattern of Fig. 1, in the neighborhood of the sharp corner near $X=0$ between the horizontal endwall and slanted sidewall, the convectively-driven flow does not fully touch the horizontal surface. This results in a lower value of Nu. In the opposite corner near $X=1.0$, the fluid vigorously washes out the walls as the flow smoothly turns around the concave surfaces of the corner. This produces a high value of Nu, and the Nu profiles of Fig. 2(a) are consistent with this physical reasoning.

Compiling the computational results, the enhancement of overall heat transfer throughout the cavity, which is shown by the mean Nusselt number at the cold bottom endwall, defined as

$$\overline{Nu}\equiv\frac{1}{2}\int\frac{\partial\theta}{\partial Y}\mathrm{d}X\bigg|_{Y=0},$$

is illustrated in Fig. 2(b). Obviously, the gain in $\overline{Nu}$ is substantial as ϕ increases, and, as anticipated, the augmentation is more conspicuous at large Ra.

Second, the cavity geometry with undulating insulating

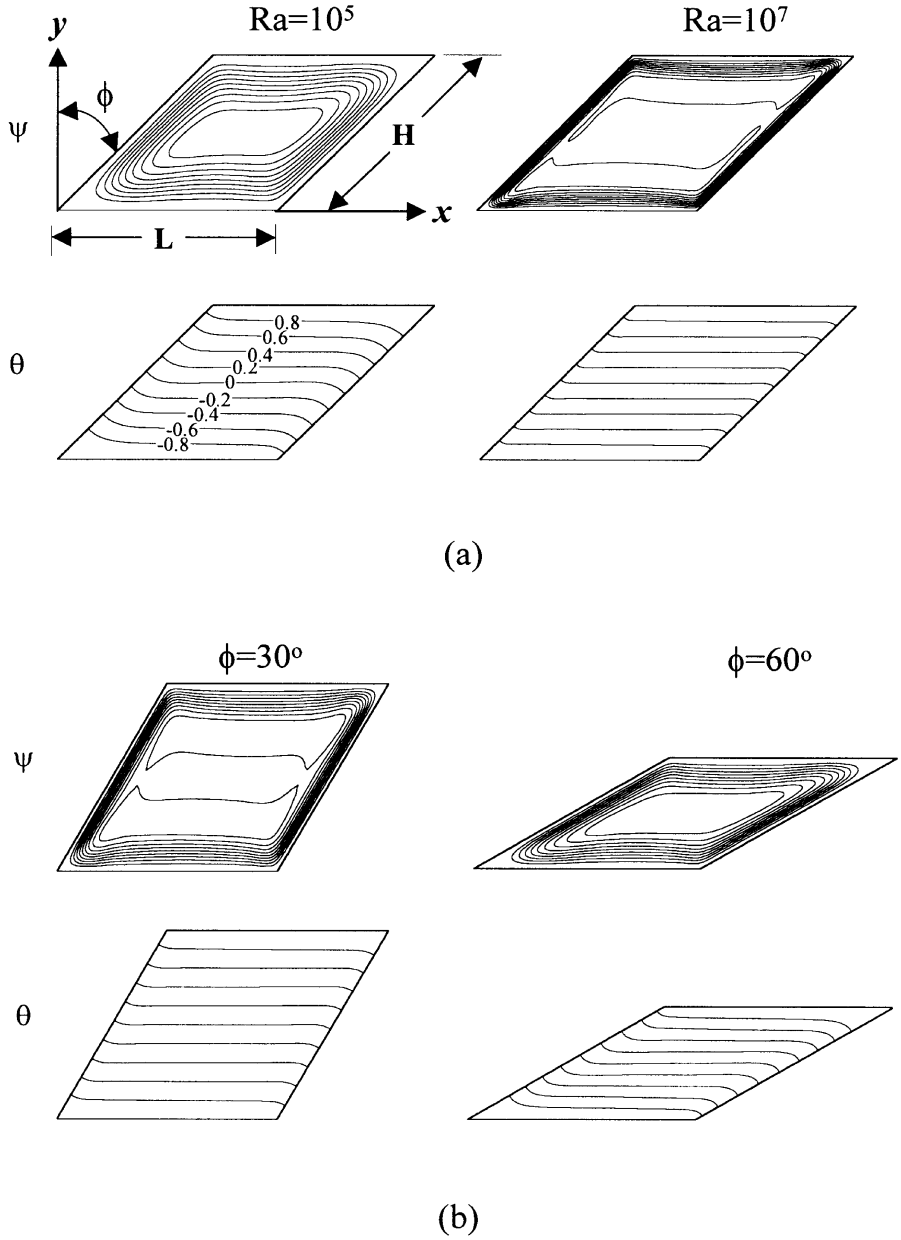

Fig. 1. Flow in a parallelogram-shaped cavity: (a) $\phi = 45^{\circ}$; (b) $Ra = 10^6$.

sidewalls will be dealt with. For an explicit mathematical representation, a sinusoidal form of nondimensional amplitude $\varepsilon\,[\equiv l/H]$ and wavelength $\eta\,[\equiv h/H]$ is selected.

Figure 3 exemplifies the changes in flow and temperature fields as Ra and the number of waves in the sidewall shape, $N\,[\equiv 1/\eta]$, are altered, while the amplitude of sidewall waviness ε is fixed at $\varepsilon = 0.1$. The results disclose that the entire cavity appears to consist of a series of overlying $2N$ mini-cavities; the flow in each mini-cavity is qualitatively similar to that in a parallelogram-shaped cavity illustrated in Fig. 1 with an effective height $\eta/2$. The corresponding incline angle ϕ of the uppermost mini-cavity is positive, producing a counter-clockwise circulation cell; for the next underlying mini-cavity, ϕ is negative, which generates a clockwise circulation cell. This alternating sequence is repeated from the top to bottom horizontal endwalls. These features are a manifestation of the afore-stressed role played by baroclinicity in the neighborhood of non-vertical sidewalls.

In order to assess the impact on the overall heat trans-

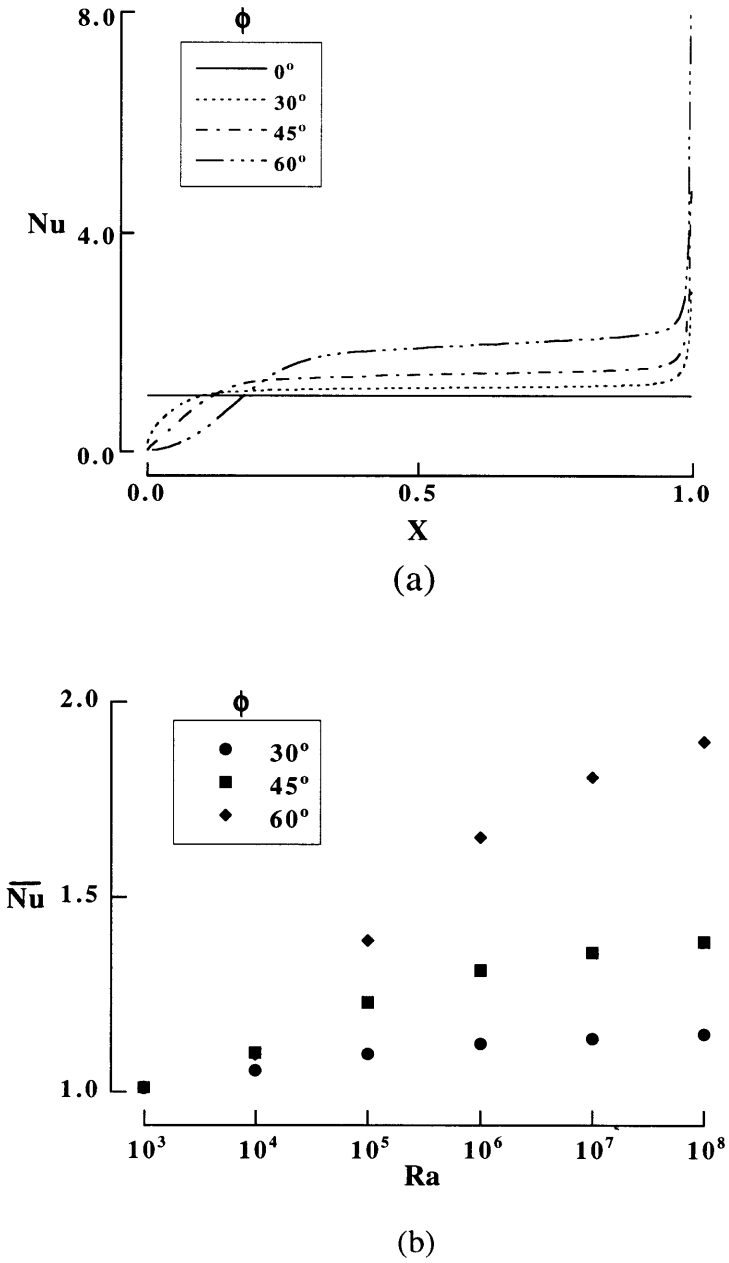

Fig. 2. Nusselt number distributions: (a) local Nusselt number at $Y = 0.0$; $Ra = 10^6$; (b) mean Nusselt number at $Y = 0.0$.

port from the top to bottom endwalls, it is advantageous to utilize the previous results pertinent to a parallelogram-shaped cavity of Fig. 1. For a mini-cavity, the effective aspect ratio $Ar_m \cong \eta/2$, the effective incline angle $\phi_m \cong \tan^{-1}(4\varepsilon/\eta)$, and the effective Rayleigh number $Ra_m \cong Ra \cdot Ar_m^4$. Since ε is fixed ($\varepsilon = 0.1$ in the present computations), it follows that, as the sidewall shape becomes more wavy, η and, consequently, Ra_m decrease but $|\phi_m|$ increases. As learned from the results for the parallelogram-shaped cavities (see Fig. 2), these two effects make qualitatively opposite contributions to the global heat transport in the vertical direction. These considerations suggest that there exists an optimal value of N to maximize the overall transfer rate. For this purpose, Fig. 4 exhibits the changes in the relative gain due to convective heat transport when $Ra \gtrsim 10^3$. The ordinate

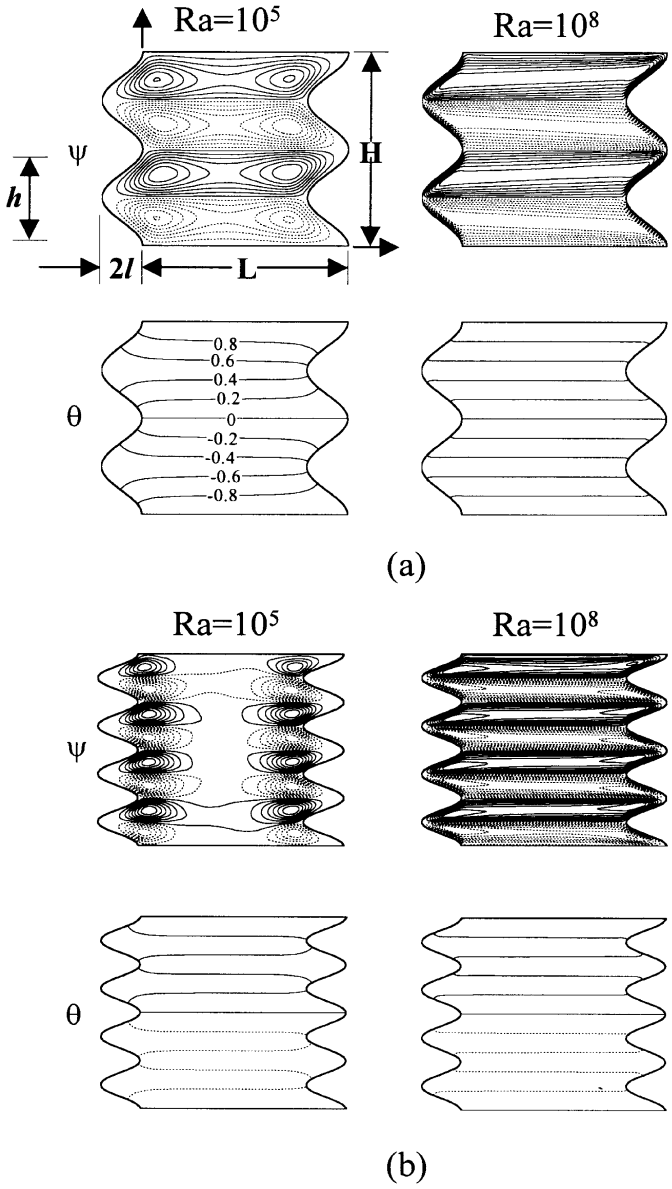

Fig. 3. Flow in a cavity with wavy sidewalls. Solid (dotted) lines denote counter-clockwise (clockwise) circulations; (a) $N = 2$; (b) $N = 4$.

of Fig. 4 shows the quantity $G \equiv \dot{Q}/\dot{Q}_{\text{cond}}$. In the above,

$$\dot{Q} \equiv \int \left(\frac{\partial \theta}{\partial Y}\right)_{Y=0} \mathrm{d}X$$

represents the actual total heat transfer rate in the present convective fluid system, and

$$\dot{Q}_{\text{cond}} \equiv \int \left(\frac{\partial \theta}{\partial Y}\right)_{Y=0} \mathrm{d}X$$

indicates the heat transport solely by conduction for the given cavity geometry. For a rectangular cavity, $\dot{Q}_{\text{cond}}$, by definition, is 2.0. However, it should be recalled that, for a non-rectangular cavity with non-vertical insulated sidewalls, $\dot{Q}_{\text{cond}}$ is not necessarily 2.0. For this case, the conductively-controlled isotherms must meet the sidewalls in the locally perpendicular direction. Therefore, the isotherms in the vicinity of the horizontal walls near the sidewalls are not perfectly parallel and equi-spaced, which makes $\dot{Q}_{\text{cond}}$ deviate from 2.0. The quantity G in

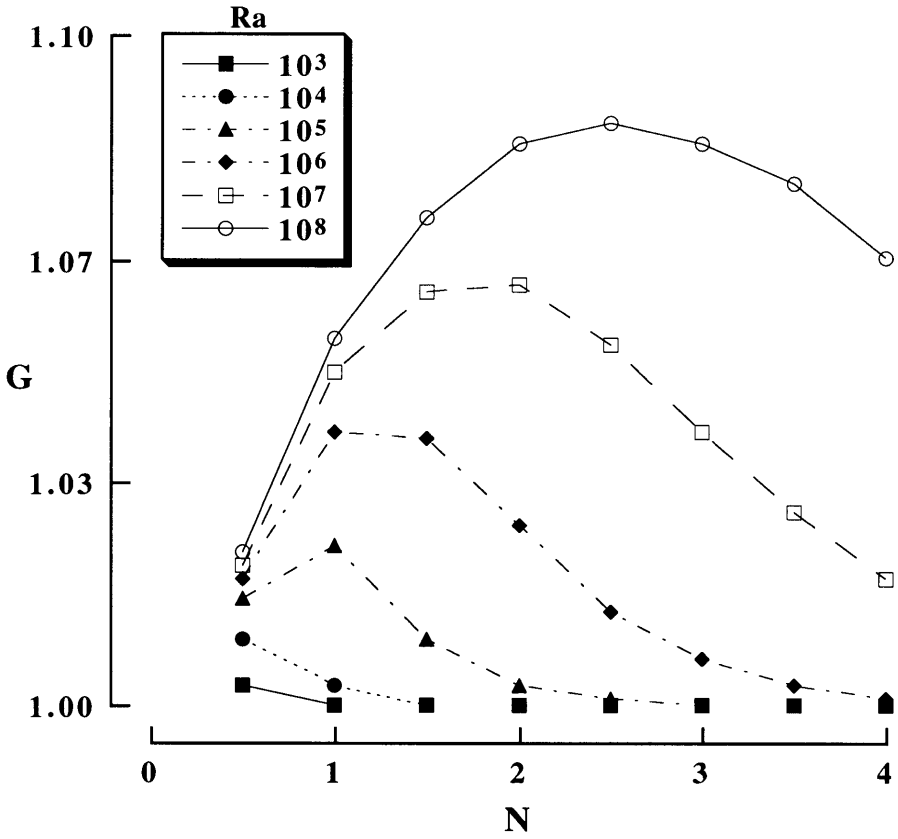

Fig. 4. Variations in convective gain in overall heat transport, G.

the present computations denotes the relative increase in actual heat transport, augmented by convective activities, over the value attainable by conduction alone for the specific geometry.

Figure 4 demonstrates that, for large Ra, say $Ra \gtrsim 10^5$, convection is the primary heat transfer mode. It is also apparent that there exists an ideal wavy form for the sidewall which would produce maximal convectively-initiated enhancement of heat transport. Obviously, the optimal number of peaks in the sinusoidal wavy sidewall shape, N, tends to increase as the nominal cavity-system Rayleigh number Ra increases.

4. Conclusion

Numerical results are scrutinized for two prototypical forms of the insulating sidewall. The key dynamical element is the flow generation by local baroclinicity in the immediate neighborhood of the non-vertical sidewalls.

For a cavity with slanted sidewalls, at high Ra, flows are concentrated to the boundary layers on the walls. For a positive incline angle ϕ, a counter-clockwise circulation cell occupies the cavity. In the interior, fluid is mostly motionless and is in a nearly-linear vertical stratification. The enhancement of global heat transfer is more pronounced as Ra and ϕ increase.

For the case of a sinusoidal wavy sidewall, the whole cavity appears to be composed of $2N$ parallelogram-shaped mini-cavities. A series of alternating counter-clockwise and clockwise circulation cells are discernible. As N increases, the effective Rayleigh number and the effective incline angle of a mini-cavity make opposite contributions to the overall heat transfer. For a fixed value of the amplitude of undulation in the sidewall shape, an optimal value of N is shown to exist which would maximize the convective gain in total heat transfer.

Acknowledgements

This work was supported in part by grants from MOST, KOSEF-RRG at Sun Moon University and the Research and Management Center for Energy and Resources, Korea.

References

[1] S. Ostrach, Natural convection heat transfer in cavities and cells, Proceedings of the Seventh International Transfer Conference, vol. 1, 1982, pp. 365–379.
[2] J.M. Hyun, Unsteady buoyant convection in an enclosure, Advances in Heat Transfer, vol. 24, Academic Press, New York, 1994, pp. 227–320.
[3] L. Iyican, Y. Bayazitogulu, L.C. Witte, An analytical study of natural convective heat transfer within a trapezoidal enclosure, J. Heat Transfer 102 (1980) 640–647.
[4] L. Iyican, Y. Bayazitogulu, L.C. Witte, An experimental study of natural convection in trapezoidal enclosures, J. Heat Transfer 102 (1980) 648–653.
[5] T.S. Lee, Computational and experimental studies of convective fluid motion and heat transfer in inclined non-rectangular enclosures, Int. J. Heat Fluid Flow 5 (1) (1984) 29–36.
[6] T.S. Lee, Numerical experiments with fluid convection in tilted non-rectangular enclosures, Numer. Heat Transfer 9 (1991) 487–499.
[7] M. Peric, Natural convection in trapezoidal cavities, Numer. Heat Transfer 24 (1993) 213–219.
[8] T. Maekawa, I. Tanasawa, Natural convection heat transfer in a parallelogrammic enclosure, Proceedings of the Seventh International Heat Transfer Conference, vol. 2, Hemisphere, Washington, D.C., 1982, pp. 227–232.
[9] J.M. Hyun, B.S. Choi, Transient natural convection in parallelogram-shaped enclosure, Int. J. Heat Fluid Flow 11 (2) (1990) 129–134.
[10] G.N. Facas, Laminar free convection in a nonrectangular inclined cavity, J. Thermophys. and Heat Transfer 7 (3) (1993) 447–453.
[11] S.V. Patankar, Numerical Heat Transfer and Fluid Flow, Hemisphere/McGraw-Hill, New York, 1980.